

Electrical properties of ZnO additive with (Al₂O₃) and (TiO₂) nano thin films

Manal Midhat Abdullah

Abstract— In this work, (ZnO)_{0.9} thin films additives with (Al₂O₃)_{0.05} and (TiO₂)_{0.05} nano particles are prepared on glass substrate under vacuum (10-5mbar) at room temperature using thermal evaporation method. The effect of annealing temperatures (100,150 200) °C on the structural and electrical properties is studied. AFM is studied to have a better idea of the surface morphology,. Also D.C. conductivity of films is studied to determine the activation energies. Hall Effect is studied to determine the type of the current carrier, Hall mobility and other Hall coefficient are regarded too. Also the transmission , the energy gap and optical properties are included .Don't use all caps for research paper title.

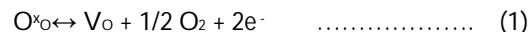
Index Terms— additive, annealing, electrical properties, hall effect semiconductor, thin film, ZnO.

1 INTRODUCTION

Although thin films have many different ways of preparation, but they all met in one feature, which is they may have a wide range of physical and chemical properties. These properties are achieved by varying the relative proportions of the components This strategy has been used to tune numerous thin film properties including refractive index [1], dielectric constant [2], lattice constant,[3] hardness [4], charge storage capacity [5] and surface roughness [6]. The ability to engineer films with specific physical characteristics impacts a broad range of technologies. These technologies include integrated circuits [5,7], optoelectronics[3,8], gas sensors [9,10], and thermal barrier coatings[11,12].

Thermal deposition technique is a useful technique for solid compound used for thin films preparation. This method relies on surface chemical reactions, these reactions typically occur by evaporating the powder mixture of components under vacuum, and depositing the vapor on a glass substrate. The resulting films are usually dense, homogeneous, and conformal to the underlying substrate. This methods also have been used previously to deposit compound films including nanolaminates [13, 14], alloys [15], complex oxides [16, 17], and doped materials [18]. Due to an increased understanding of size-dependent nanoparticle properties and probable applications, an increasing demand for synthesis methods for the formation of specific nanoparticles with tuned properties has evolved. this introduction addresses different possibilities for the formation of nanomaterials with specific properties : Semiconducting oxide nanoparticles such as tin oxide and zinc oxide are seriously discussed as transparent conducting oxides (TCOs) for the formation of transparent conducting layers as they are used in flat panel displays and solar cells, while titanium is used as the electron-conducting electrode in dye solar cells, the so-called Grätzel cells. Up to now, the market for TCOs has been dominated by indium tin oxide (ITO) and fluorine-doped tin oxide (FTO), mainly prepared by chemical vapor deposition (CVD), physical vapor deposition (PVD) and sputtering. These methods usually require expensive, low-pressure process steps and have the disadvantage that a lot of the material is not deposited on the substrates but is lost as so-

called off-spray. Printing methods using nanoparticles such as ink-jet printing or roll-to-roll printing would allow minimizing the waste of the TCO, but these methods are still not able to completely resolve the issue of the high cost of ITO [7]. In addition, the electrical as well as the optical performance of printed layers based on nanoparticles mostly do not meet the requirements for TCO layers. This is mainly due to the following drawbacks: (1) Agglomerates and bigger nanoparticles exceeding a size of about 1/10th of the wavelength of the visible light decrease the transparency .(2) The electrical properties of the printed films is poor compared to a common layer prepared by CVD or PVD due to poor electrical properties of the particles themselves as well as to poor particle-particle contacts. (3) Almost all oxide semiconductors are n-type conductors, which means that the majority charge carriers are electrons. The electrons in the oxides originate from oxygen that is released from the lattice leaving behind two charge carriers, and can be described by the Kröger-Vink notation [19].



As a result, the adjustment of specific properties with respect to the electrical properties requires a tuning of the particle composition, especially its oxygen content during particle formation.

In present work, we studied effect of adding ZnO thin films to (Al₂O₃) and (TiO₂) nanoparticles, thermally evaporated on glass substrate at room temperature to form thin filmed samples.

As the annealing plays a significant rule on the structural and electrical properties, we annealed our samples at temperatures (100,150 and 200)°C . then different studies and investigations are studied.

2 THEORY

Zinc oxide is an inorganic White solid compound with the formula ZnO. ZnO is a white powder that is insoluble in

water, which is widely used as an additive in numerous materials and products including plastics, ceramics, glass, cement, lubricants, paints, ointments, adhesives, sealants, pigments, batteries, ferrites, fire retardants, and first aid tapes. It has a wide, direct band gap of 3.3eV this advantages associated with a large band gap include higher breakdown voltages, ability to sustain large electric fields, lower electronic noise, and high-temperature and high-power operation[20]. The band gap of ZnO can further be raised to show better features. ZnO also has several favorable properties, such as good transparency, high electron mobility, and strong room-temperature luminescence. Those properties are used in emerging applications for transparent electrodes in liquid crystal displays, in energy-saving or heat-protecting windows, and in electronics as thin-film transistors and light-emitting diodes.

The change of electrical conductivity with temperature of semiconductors are given by the equation:

$$\sigma = \sigma_0 \exp(-E_a/k_B T) \quad \dots\dots\dots (2)$$

where E_a is the thermal activation energy, T is the absolute temperature, k_B is the Boltzmann constant and σ_0 is the minimum metallic conductivity (the value of σ when $(1/T) \rightarrow \infty$). Petritz and others had suggested a model for the electrical conductivity of polycrystalline films where the conduction in the low temperature range take place through hopping because there is no sufficient energy to transport the charge carriers to another adjacent atoms, thus the carrier hops between the atoms located at the same energy, in polycrystalline materials hopping take place at the grain boundaries. At high temperature the conduction occurs as a results of transporting of charge carriers thermally through the grain boundaries. The energies for direct electron transitions are determined from the well known Tauc equation:

$$\alpha h\nu = B (h\nu - E_g)^r \quad \dots\dots\dots (3)$$

Where α is the absorption coefficient, B is a coefficient of proportionality, $h\nu$ is the energy of the light, E_g is the band gap of the material.

3 EXPERIMENTAL

Thermal evaporation technique under vacuum is used to prepare samples. 0.9 gm of ZnO Powder, is added to 0.05 gm of Al_2O_3 powder and 0.05 gm of TiO_2 powder. The powder mixture is evaporated on a cleaned glass substrates. Molybdenum boat is used for this purpose. System is evacuated down to 10^{-5} mbar; an electric current is passed through the boat gradually. Deposition process starts with constant deposition rate equal to 1.25 nm/ sec. then the current supply is switched off and the samples are left under the vacuum, then the air is admitted to the chamber, the films are taken out from the coating unit and kept in the vacuum desiccators until the measurements are made. all samples are prepared under same conditions (pressure, substrate, temperature and rate of deposition). The main parameter that

controls the nature of the film is the annealing temperature, we choose (303, 373 and 423)K for this purpose. For the electrodes needed for electric measurements, we made suitable masks from Aluminum foil, width 1 cm and distance between electrodes of (0.1 cm).

The samples thicknesses are measured by using the equation:

$$t = \frac{m}{\rho A} \quad \dots\dots\dots (4)$$

Where t is the film thickness, m is the mass of the material to be evaporated, h is the boat to substrate distance, and ρ is the density of the materials to be evaporated.

The electrical conductivity (D.C. conductivity) has been measured as a function of temperature for the films over the range (room temp. - 423 K). Measurements are conducted by a sensitive digital electrometer type Keithley (616) and electrical oven.

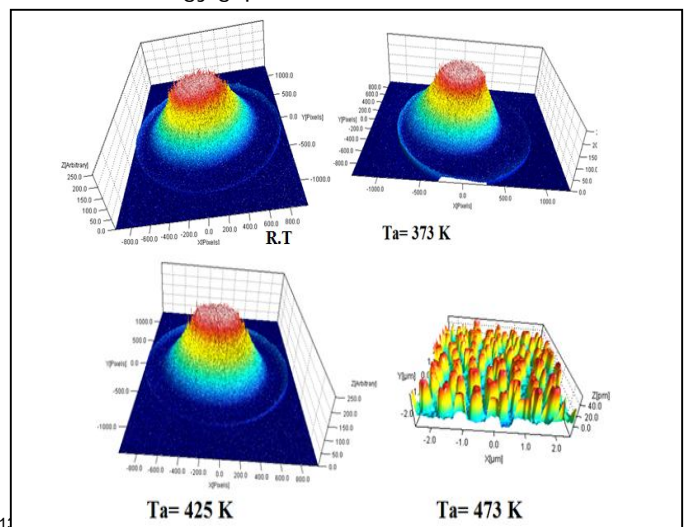
Hall effect measurements are carried out according to the well known electric circuit, the circuit contains a D.C. power supply with 0- 40 volts and two digital electrometer type Keithley (616) to measure the current and the voltage. When the magnetic field ($B = 0.55$ Tesla) is applied perpendicular to the electrical field, a transverse e.m.f (Hall voltage V_H) is set up across the sample.

Metrology scanning probe is applied to show the surface condition, also AFM test is used to analyze the surface morphology.

4 RESULTS AND DISCUSSION

Figure (1) shows surface image pictures of samples before and after annealing, a- images taken by optical microscope, the spots denotes the additives (Al_2O_3) and (TiO_2). b- surface scan studied by metrology scanning probe, the scale is 11nm/pixel.

Figure (2) shows the variation of particles mean heights as a function of annealing temperatures for studied samples by metrology scanning probe software. It can be declared that the particles size increase with increasing of annealing temperatures. This is due to the growth of grain size and the decrease in defect states near the bands and in turn increased the values of Energy gaps.



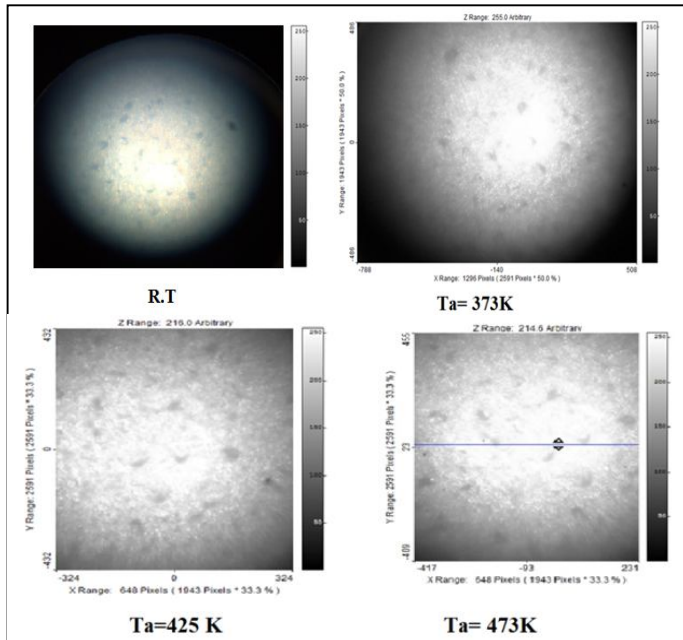


Figure (1): a- microscope surface image pictures for the samples before and after annealing. b- metrology scanning probe analysis of the samples.

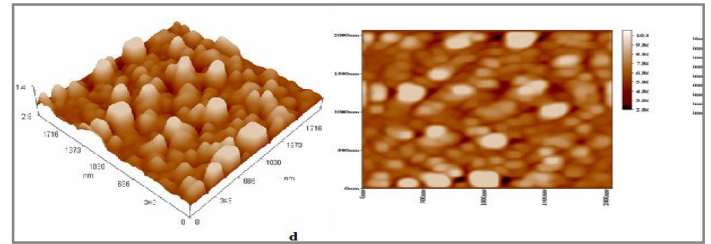


Fig.2 shows two and three-dimensional image for ZnO thin film additive under different annealing temperatures obtained by AFM analysis.

AFM analysis is declared in figure 3 for ZnO thin film additive under different annealing temperatures. comparing the three dimensional figures (a,b,c and d)for figure 3, we can clarify the growing up peaks on the sample surface with increasing the annealing temperature.

It is obvious that the particle mean height and accordingly surface roughness average showed direct proportionality with increasing the annealing temperature, this is attributed to the crystalline of the films under annealing treatment. this behavior is shown in figures 3 and 4.

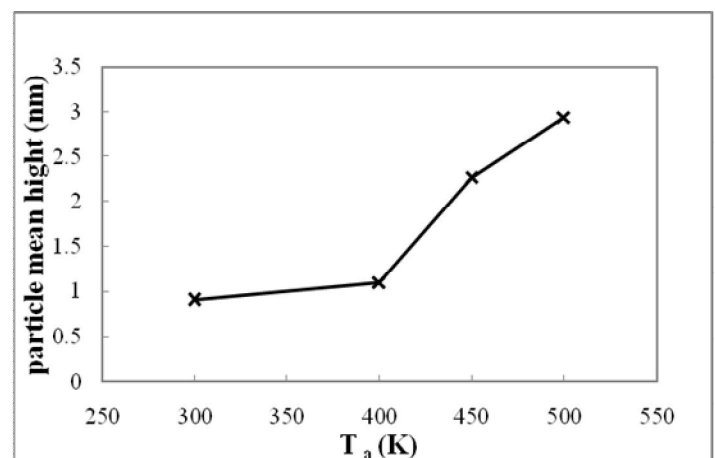
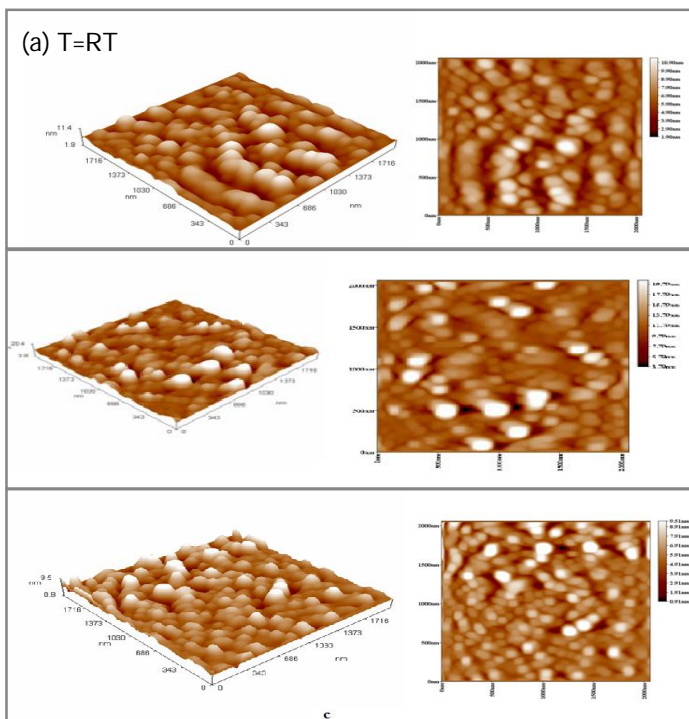


Fig.(3) variation of particles mean high as a function of annealing temperature.

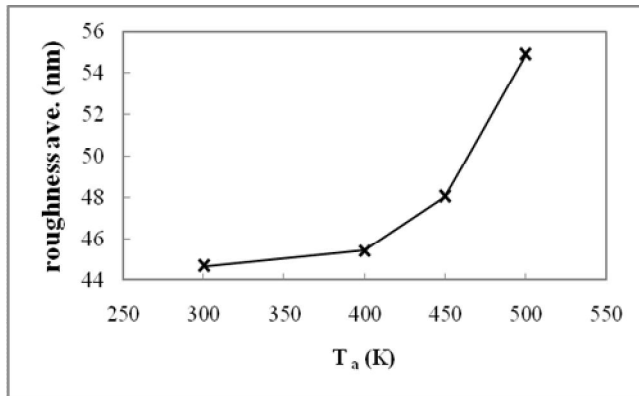


Fig.(4) surface roughness vs. annealing temperature.

The variation of The plots of $\ln \sigma$ versus $10^3/T$ for ZnO thin film additive at different annealing temperatures is shown in figure 5. It is clear from this figure that there are two transport mechanisms, giving rise to two activation energies E_{a1} and E_{a2} . The conduction mechanism of the activation energy (E_{a2}) at the higher temperatures range (403-493)K is due to carriers excitation into the extended states beyond the mobility edge and at the lower range of temperatures (303-393)K, the conduction mechanism is due to carriers excitation into localized state at the edge of the band [21]. Table (1) show the effect of annealing temperature on both activation energies E_{a1} and E_{a2} for films. It is clear that the activation energies decrease with increasing of annealing temperatures.

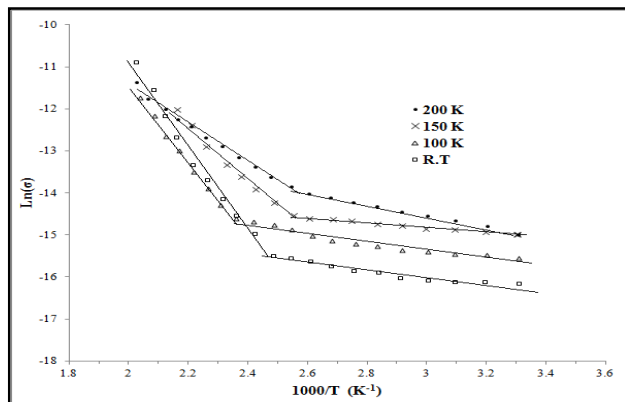


Fig.(5) $\ln(\sigma)$ versus $1000/T$ for ZnO additive with Al_2O_3 and TiO_2 films at different annealing temperatures.

Table(1): The values of activation energies for ZnO additive with Al_2O_3 and TiO_2 films at different annealing temperatures.

T _a (K)	E _{a1} (eV)	Range(K)	E _{a2} (eV)	Range(K)
R.T	0.073	303-403	0.809	403-483
373	0.083	303-423	0.784	423-493
425	0.049	303-393	0.555	393-463
473	0.115	303-393	0.411	393-493

The Hall measurements that includes Hall mobility, carrier type and concentration for as-deposited ZnO additive with Al_2O_3 and TiO_2 films and heat treatment at (RT, 373, 425 and 473)K were measured from Hall coefficient (R_H) data and D.C. conductivity.

Hall measurements show that the films are n-type i.e., the conduction is dominated by electrons. This is obviously due to the excess of the ratio of ZnO which may produce excess electrons in the films. From the carrier concentration, the results are listed in Table (2).

Table (2) values of Hall effect measurements for ZnO additive with (Al_2O_3) and TiO_2) thin film at different annealing temperatures.

T _a (k)	R _H (cm ³ /c)	n _H (cm ⁻³)	σ _{RT} (Ωcm) ⁻¹	type	μ _H (cm ² /v.s ec)
R.T	-18.2*10 ⁶	3.43*10 ¹¹	4.02*10 ⁻⁶	n	73.3
373	-6.9*10 ⁶	9.03*10 ¹¹	6.65*10 ⁻⁶	n	46.0
423	-5.9*10 ⁶	10.5*10 ¹¹	7.40*10 ⁻⁶	n	44.1
473	-7.52*10 ⁶	8.31*10 ¹¹	5.79*10 ⁻⁶	n	43.5

The increase in the conductivity with temperature is obviously due to the increases in the carrier concentration and absorbance. We can notice from the above table that the mobility decreases (for pure ZnO, the electron mobility at T = 300 K is 200 cm²/V sec[22], while the carriers concentration increases with increasing of annealing temperatures, and this is attributed to either increasing the trapping centers [23] or the films may have a large amount of adsorbed oxygen which reduces both the number of charge carriers and their mobility essentially because of the higher grain boundary barrier height [24].

The transmittance spectrum of films in the spectral range (300-800)nm at room temperature is shown in figure 6. In general, we can observe that the transmittance increases with increasing of wavelength which means a decrease in the reflection and absorption. the films show low transparent at lower wavelength and higher transparent films about 70% occur in the visible region.

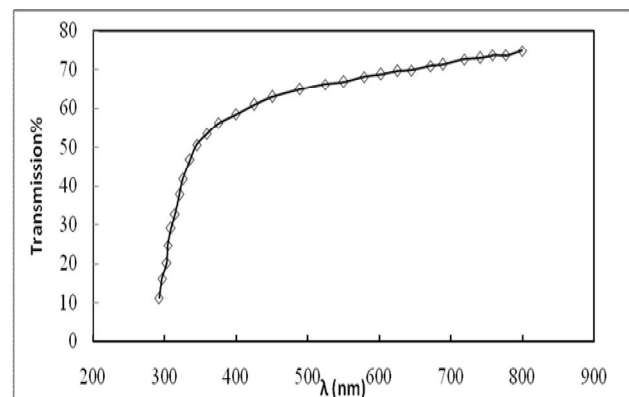


Figure 6: The transmission spectrum of films in the spectral

range (300-800)nm at room temperature.

In calculating the absorption coefficient in the region of the fundamental absorption edge for ZnO additive thin films, we plot of the absorption coefficient vs. wavelength in the strong absorption edge give details on the shape of absorption edge of films.

Figs(7) shows the absorption coefficient of films vs. wavelength in the range of (300-800)nm at RT. From this figure, the absorption spectra are characterized by strong absorption at short wavelength within the range (300-370)nm with a sharp edge on the long wavelength side within the range (370-800)nm. In the short wavelength, the absorption coefficient takes higher values ($>10^4 \text{cm}^{-1}$) indicating that the transition in the films is direct transition and then α is decreased sharply with the increasing of wavelength, and beyond that the change becomes slight, this sharp or low increment is attributed to the lattice absorption bands correspond to the electronic transitions between the highest filled energy band to the lowest empty band also corresponds to the density of absorbing centers such as impurities absorption, excitation transition, and other defects in the crystal lattice dependent on the conditions of sample.

It is found from figure 8 that the value of energy gap for ZnO additive with (Al_2O_3) and (TiO_2) equal to 3.95 eV, (while the pure ZnO has $E_g = 3.3 \text{ eV}$).

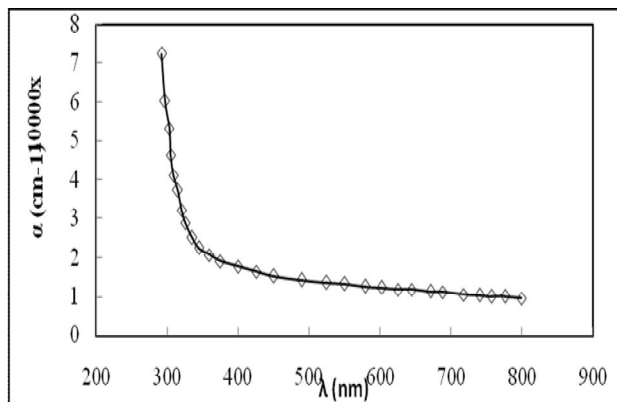


Figure .(7) The variation of the absorption coefficient with wavelength for ZnO additive with (Al_2O_3) and (TiO_2).

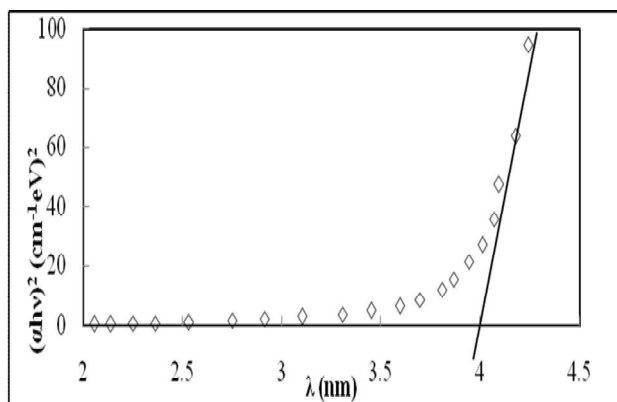


Figure .(8) The variation of $(\alpha h\nu)^2$ with photon energy for

ZnO additive with Al_2O_3 and TiO_2 films.

Using Eq. $k = \frac{4\pi}{\lambda} \alpha$, we can obtain the dependence of extinction coefficient on wavelength. The behavior of k is similar to that correspondent to the absorption coefficients. It is clearly evident that k decreases with increasing of wavelength as shown in figure 9.

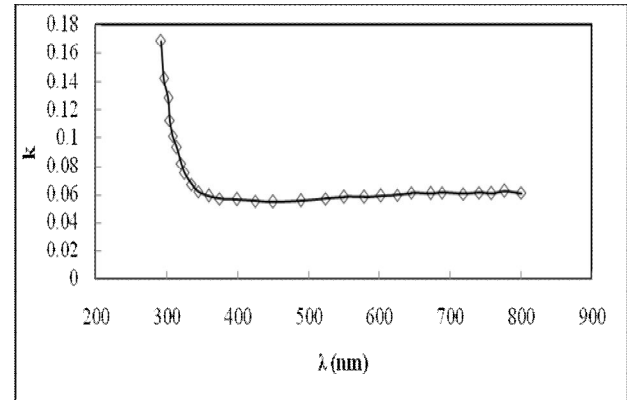


Figure.(9) shows the Extinction coefficient (k) as a function of wavelength for ZnO additive with (Al_2O_3) and (TiO_2) thin film at different annealing temperatures.

5 CONCLUSION:

ZnO has a relatively large direct band gap of $\sim 3.3 \text{ eV}$ at room temperature, in this paper we increased this value to 3.95 eV by adding additives (Al_2O_3) and (TiO_2).the particle mean height and the surface roughness average are increased with increasing the annealing temperature. Also the carriers concentration and the conductivity increases with increasing annealing temperature due to the increases in the carrier concentration and absorptance. While mobility decreases while increases with increasing of annealing temperatures, and this is attributed to increasing the trapping centers.

6 REFERENCES

- [1] H. Kattelus, M. Ylilammi, J. Saarilahti, J. Antson, and S. Lindfors, Thin Solid Films, 225, 296 -1993.
- [2] M. Stromme, G. A. Niklasson, M. Ritala, M. Leskela, and K. Kukli, J. Appl. Phys.,90, 4532-2001.
- [3] H. Fujiwara, T. Nabeta, and I. Shimizu, Jpn. J. Appl. Phys., Part 1, 33, 2474-1994.
- [4] X. Chu, M. S. Wong, W. D. Sproul, and S. A. Barnett, J. Mater. Res., 14, 2500-1999.
- [5] K. Kukli, M. Ritala, and M. Leskela, J. Appl. Phys., 86, 5656-1999.
- [6] J. W. Elam, Z. A. Sechrist, and S. M. George, Thin Solid Films, 414, 43 -2002.

- [7] M. Vehkamäki, T. Hatanpää, T. Hanninen, M. Ritala, and M. Leskela, *Electrochem. Solid-State Lett.*, 2, 504 - 1999.
- [8] J. Ihanus, M. Ritala, M. Leskela, and E. Rauhala, *Appl. Surf. Sci.*, 112, 154 -1997.
- [9] H. Y. Bae and G. M. Choi, *Sens. Actuators B*, 55, 47 -1999.
- [10] J. H. Yu and G. M. Choi, *Sens. Actuators B*, 75, 56 -2001.
- [11] S. Sharafat, A. Kobayashi, V. Ogden, and N. M. Ghoniem, *Vacuum*, 59, 185-2000.
- [12] F. Wang, L. Wang, and G. Liu, *Surf. Eng.*, 17, 35-2001.
- [13] M. Ritala, M. Leskela, L. Niinisto, T. Prohaska, G. Friedbacher, and M. Grasserbauer, *Thin Solid Films*, 249, 155-1994.
- [14] K. Kukli, J. Ihanus, M. Ritala, and M. Leskela, *Appl. Phys. Lett.*, 68, 3737 -1996.
- [15] H. Zhang and R. Solanki, *J. Electrochem. Soc.*, 148, F63-2001.
- [16] M. Nieminen, T. Sajavaara, E. Rauhala, M. Putkonen, and L. Niinisto, *J. Mater. Chem.*, 11, 2340 -2001.
- [17] A. Rahtu, T. Hanninen, and M. Ritala, *J. Phys. IV*, 11, 923 -2001.
- [18] E. B. Yousfi, B. Weinberger, F. Donsanti, P. Cowache, and D. Lincot, *Thin Solid Films*, 387, 29 -2001.
- [19] Hartmut Wiggers, notes on novel material properties based on synthesized nanopowder technology, Institut für Verbrennung und Gasdynamik, University Duisburg-Essen, 2009,
- [20] J. Pearton, D. P. Norton, K. Ip, Y. W. Heo, T. Steiner, *Prog. Mater. Sci.* 50, 293 - 2005.
- [21] M Orita, H Ohta, M Hirano, H Hosono, *App Phys Lett* 77 4166- 2000.
- [22] ZHIYONG FAN AND JIA G. LU, *JOURNAL OF NANOSCIENCE AND NANOTECHNOLOGY*, 5, 10, PP. 1561-1573(13) , OCTOBER 2005
- [23] SHARMA,, *PARMANAND JOURNAL OF APPLIED PHYSICS*, 93 , 7 , 3963 – 3970, APR 2003
- [24] P.Paiano, P.Prete, N.Lovergine, and A.M.Mancini, *Cryst. Res. Technol.* Vol. 40, No.10-11, pp1011-1017, 2005.

S